

Swing-up Control for an Inverted Pendulum with Restricted Cart Rail Length

Ji-Hyuk Yang, Su-Yong Shim, Jung-Hun Seo, and Young-Sam Lee*

Abstract: In this paper, we propose a new swing-up strategy for cart inverted pendulums with restricted rail length. The proposed swing-up strategy is derived from a new Lyapunov function. The Lyapunov function is defined as the sum of the square of the pendulum energy and the weighted square of the cart's velocity. The resulting swing-up strategy is represented in a compact form and has two design parameters. By adjusting these design parameters, we can affect the swing-up strategy such that the restriction on the rail length is satisfied. We also provide a state-dependent transformation to obtain voltage input to a DC motor required to generate the cart's acceleration obtained from the proposed swing-up strategy. Finally, we illustrate the performance of the proposed swing-up law through simulation and experiments. It is shown that there is quite good correspondence between theory and experiments.

Keywords: Cart inverted pendulum, restricted rail length, state-dependent transformation, swing-up strategy.

1. INTRODUCTION

Pendulums are widely used in nonlinear control education and research as benchmark examples of underactuated mechanical systems. Extensive research can be found on the control of inverted pendulums and, in particular, swing-up control of inverted pendulums has attracted much attention. A fundamental method of swinging up cart pendulum systems is based on energy methods [1,2]. This method works well when the available cart rail length is unlimited, which is not the case with the usual cart pendulum systems.

In the literature available, there are several solutions for swing-up stabilization of cart pendulums with a restricted rail. Wei *et al.* [3] presented a nonlinear control strategy by decomposing the control law into a sequence of steps. Chung and Houser [4] proposed a nonlinear state feedback control law to regulate the cart position as well as the swinging energy of the pendulum. Lozano *et al.* [5] used a Lyapunov function to derive a swing-up law taking restricted rail length into account. The Lyapunov function is given by the sum of the squares of mechanical energy, cart position and cart velocity. The resultant swing-up law has four parameters, which requires a trial and error tuning procedure. Furthermore, the swing-up is relatively sluggish as illustrated in simulations and experiments in the paper. Zhao and Spong [6] applied a hybrid-control strategy, which

globally asymptotically stabilizes the system for all initial conditions. Their swing-up strategy consists of switching between bang-bang controllers and requires a lot of parameters to be decided upon. Their method does not take the rail length restriction into account. Chatterjee *et al.* [7] introduced the concept of "potential well" in order to consider the cart rail length limitation. The well is constructed in such a way that the cart experiences a repulsive force as it approaches the boundaries in the neighborhood of the limitations. The simulation and experimental results given in the paper show that their method is effective. However, a major problem with their method is to design suitable potential wells and coefficients using intuition and time-consuming iterations. Five coefficients should be designed by trial and error, which is not easy. A fuzzy swing-up algorithm was applied in [8]. However, it is difficult to prove the stability of the control systems based on a fuzzy algorithm. Furthermore, trial-and-error approaches should be taken to complete the fuzzy algorithm. Swing-up control of a rotary inverted pendulum known as a Furuta pendulum has also been presented in [9]. The method presented in [9] is obtained by applying Fradkov's speed-gradient method to a dimension 4 model of the system, while the existing method [2] is based on a dimension 2 model.

In this paper, a new swing-up strategy is proposed based on a new Lyapunov function, which is given by the sum of the square of mechanical energy and weighted square of the cart's velocity. The proposed control law is represented in a simple form when compared to existing methods. It has only two design parameters and thus is easy to tune and is clearly an advantage over existing methods which require four or more parameters to be tuned. Stability is guaranteed irrespective of the choice of design parameters as long as the values are strictly positive. Furthermore, the rail length limitation can be

Manuscript received March 4, 2008; revised October 25, 2008; accepted February 7, 2009. Recommended by Editorial Board member Duk-Sun Shim under the direction of Editor Jae Weon Choi. This work was supported by an Inha Research Grant.

Ji-Hyuk Yang, Su-Yong Shim, Jung-Hun Seo, and Young-Sam Lee are with the School of Electrical Engineering, Inha University, 253 Yonghyun-dong, Incheon, Korea (e-mails: {zero1zuck, syong82, kensin2k1}@hanmail.net, lys@inha.ac.kr)

* Corresponding author.

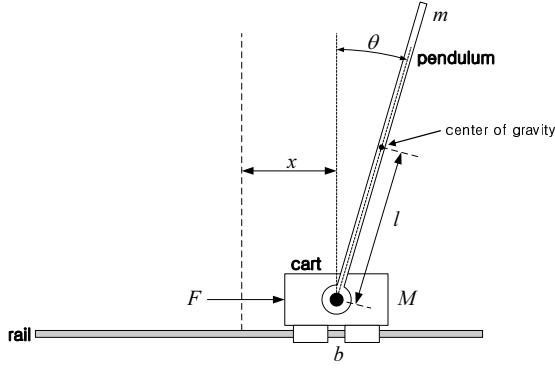


Fig. 1. The conceptual diagram of a cart pendulum system.

taken into account by adjusting the design parameters. The swing-up time of the proposed method is much shorter than that of [5] and is comparable to that of [7].

This paper is organized as follows: In Section 2, a mathematical model of a cart inverted pendulum is provided. In Section 3, a new swing-up strategy is proposed and its stability is proved. In Section 4, a state-dependent transformation is proposed in order to implement the proposed swing-up strategy in cart pendulum systems which utilize a DC motor as an actuator. In Section 5, simulation and experimental results are provided. Finally in Section 6, conclusions are made.

2. MODEL OF CART INVERTED PENDULUMS

Fig. 1 shows the conceptual diagram of a cart pendulum system. Applying Lagrange's formulation, we obtain the following differential equations which govern the movement of the pendulum system:

$$\bar{I}_p \ddot{\theta} + ml(\cos \theta) \ddot{x} - mgl \sin \theta = 0, \quad (1)$$

$$(M + m) \ddot{x} - ml(\sin \theta) \dot{\theta}^2 + ml(\cos \theta) \ddot{\theta} + b \dot{x} = F, \quad (2)$$

where $\bar{I}_p = I_p + ml^2$, I_p is the moment of inertia of a pendulum with respect to the center of gravity, M the mass of a cart, m the mass of a pendulum, l the length of the pendulum from the pivot to the center of gravity, g the acceleration of gravity, F the force exerted on the cart. The angular displacement θ and the linear displacement x are depicted in Fig. 1. We do not provide a detailed derivation procedure of the model because the modeling procedure is well known.

3. STABILIZING SWING-UP STRATEGY

From (1), if $\ddot{x} = 0$ or equivalently \dot{x} is constant, the pendulum movement is governed by the differential equation

$$\bar{I}_p \ddot{\theta} - mgl \sin \theta = 0. \quad (3)$$

As in [2], we define the energy of the pendulum as

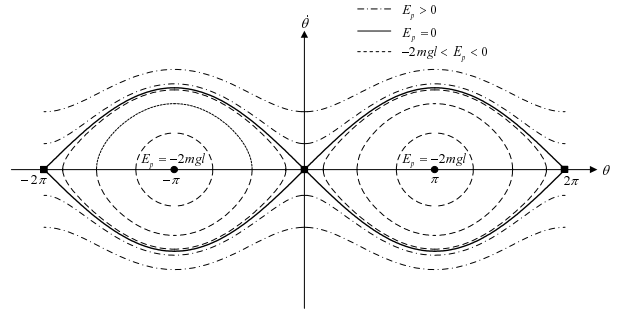


Fig. 2. Orbit of $(\theta, \dot{\theta})$ satisfying $E_p = \text{constant}$.

follows:

$$E_p = \frac{1}{2} \bar{I}_p \dot{\theta}^2 + mgl(\cos \theta - 1).$$

It is mentioned that trajectories $(\theta, \dot{\theta})$ that are solution to the differential equation (3) construct orbits satisfying $E_p = \text{constant}$. Fig. 2 depicts orbits for different values of E_p . Each orbit suffices to be an invariant set because all solutions to (3) with initial conditions in the orbit remain in the orbit. E_p has its minimum value of $-2mgl$ at the points $(\theta, \dot{\theta}) = (\pm\pi, 0)$, denoted by black circles in Fig. 2. Those points correspond to the stable equilibrium of the differential equation (3). We are especially interested in an orbit represented by $E_p = 0$, i.e.,

$$\frac{1}{2} \bar{I}_p \dot{\theta}^2 + mgl(\cos \theta - 1) = 0 \quad (4)$$

because E_p is zero when the pendulum is in the upright position. See the orbit drawn in a solid line in Fig. 2. Points denoted by black squares in Fig. 2 correspond to the upright position or unstable equilibrium. Therefore, if a swing-up strategy can make \dot{x} converge to a constant and E_p approach zero, the state trajectory $(\theta, \dot{\theta})$ will approach the orbit represented by (4), which implies that the pendulum approaches the upright position as time passes. In order to balance the pendulum at the upright position, the control is switched to a local linear controller that guarantees local asymptotic stability. Since the rail length is restricted, the most appropriate constant value which \dot{x} converges to should be zero. Otherwise, the swing-up strategy is very likely to violate the rail length restriction during its swing-up action. In order to make E_p and \dot{x} approach zero, we propose a Lyapunov function candidate as follows:

$$V = \frac{1}{2} (E_p^2 + m\lambda \dot{x}^2), \quad (5)$$

where $\lambda > 0$ is a design parameter. In order to derive a swing-up strategy, we first compute the derivative of V with respect to time as follows:

$$\begin{aligned}
\frac{dV}{dt} &= E_p \dot{E}_p + ml\lambda\ddot{x} \\
&= E_p [\bar{I}_p \ddot{\theta} - mgl \sin \theta \dot{\theta}] + ml\lambda\ddot{x} \\
&= -E_p ml \cos \theta \dot{\theta} \ddot{x} + ml\lambda\ddot{x} \\
&= -\ddot{x} ml (E_p \cos \theta \dot{\theta} - \lambda \dot{x}).
\end{aligned}$$

It is mentioned that (1) is used in order to replace the term $\bar{I}_p \ddot{\theta}$ in the above derivation. We consider the acceleration of a cart as a control variable, that is, $u = \ddot{x}$ as in [2]. Let us take the control

$$u = u_a (E_p \cos \theta \dot{\theta} - \lambda \dot{x}), \quad (6)$$

where $u_a > 0$ is a design parameter. Then dV/dt reduces to

$$\frac{dV}{dt} = -mlu_a (E_p \cos \theta \dot{\theta} - \lambda \dot{x})^2. \quad (7)$$

If V converges to zero, then $E_p \rightarrow 0$ and $\dot{x} \rightarrow 0$. This, in turn, implies that the trajectory of a pendulum approach the orbit given by (4). Switching to a local linear controller when the pendulum approaches the upright position fulfills the swing-up control. However, it is noted that $dV/dt \leq 0$ because the term $(E_p \cos \theta \dot{\theta} - \lambda \dot{x})$ can be zero in some cases. Because dV/dt is just a negative semidefinite, we need to prove that V converges to zero. The following theorem provides this proof.

Theorem 1: Consider the inverted pendulum system represented by (1) and (2). If the acceleration of the cart is given by (6) for strictly positive constants u_a and λ , then the solution of the closed-loop system with all initial state conditions other than $(\theta, \dot{\theta}) = (\pm\pi, 0)$ converges to the invariant set M represented by the orbit corresponding to $E_p = 0$ with $\dot{x} = 0$.

Proof: The stability is based on LaSalle's invariance theorem [10]. In order to apply LaSalle's theorem we need to define a compact (closed and bounded set) Ω with the property that every solution of the system given by (1) and (2) which starts in Ω remains in Ω for all future time. Since $V(\theta, \dot{\theta}, \dot{x})$ in (5) is a non-increasing function from (7), then θ , $\dot{\theta}$, and \dot{x} are bounded. The set Ω is defined as

$$\Omega = \{(\theta, \dot{\theta}, \dot{x}) \in \mathbf{R}^3 \mid V(\theta, \dot{\theta}, \dot{x}) \leq V(\theta(0), \dot{\theta}(0), \dot{x}(0))\}.$$

Therefore, the solutions of the closed-loop system remain inside a compact set Ω . Let Γ be the set of all points in Ω such that $V(\theta, \dot{\theta}, \dot{x}) = 0$. Let M be the largest invariant set in Γ . LaSalle's theorem ensures that every solution starting in Ω approaches M as $t \rightarrow \infty$. Let us now compute the largest invariant set M in Γ . All points in Γ satisfies $\dot{V} = 0$, which

corresponds to $(E_p \cos \theta \dot{\theta} - \lambda \dot{x}) = 0$. Since $M \subset \Gamma$, all points in M also satisfies $(E_p \cos \theta \dot{\theta} - \lambda \dot{x}) = 0$. Since all solutions starting in M remain in M by definition, the acceleration u also remains as zero in M from (6) and thus the closed-loop system satisfies the differential equation (3). As mentioned previously, solutions to (3) are represented by orbits satisfying $E_p = \text{constant}$, each of which suffices to be a invariant set. We will show that the orbit represented by $E_p = 0$ and $\dot{x} = 0$ is the largest invariant set M . We will consider two cases.

• **Case a:** $E_p \cos \theta \dot{\theta} = 0$ and $\dot{x} = 0$.

$E_p \cos \theta \dot{\theta} = 0$ implies that $E_p = 0$ or $\cos \theta \dot{\theta} = 0$ with $E_p \neq 0$. The set of points satisfying $E_p = 0$ corresponds to the orbit given by (4) and thus suffices to be invariant. $\cos \theta \dot{\theta}$ cannot remain zero around any orbit given by $E_p = c$, where c is not zero. The only exception is the case when $E_p = -2mgl$ which corresponds to $(\theta, \dot{\theta}) = (\pm\pi, 0)$. This implies that $(\theta, \dot{\theta}) = (\pm\pi, 0)$ can be an invariant set. However, the theorem excludes cases where the initial condition starts from $(\theta, \dot{\theta}) = (\pm\pi, 0)$. Therefore, the orbit corresponding to $E_p = 0$ is the biggest invariant set for Case a.

• **Case b:** $E_p \cos \theta \dot{\theta} = \lambda \dot{x} = c$, where c is a constant which is not zero.

The reason why we take \dot{x} to be constant is because $u = \ddot{x} = 0$ in M from (6). As already mentioned, all solutions to (3) correspond to orbits represented by $E_p = \text{constant}$. However $\cos \theta \dot{\theta}$ cannot remain constant around any specific orbit. Therefore, $E_p \cos \theta \dot{\theta}$ cannot remain constant around any specific orbit. This implies that there is no invariant set for Case b.

From the above discussion, we can conclude that the biggest invariant set M is the orbit represented by $E_p = 0$ with $\dot{x} = 0$. Since we have found the biggest invariant set M , the remaining proof follows from LaSalle's theorem. This completes the proof.

Remark 1: Lozano's method [5] requires four design parameters to be tuned. It is reported that a major problem with the method in [7] is to design suitable potential wells and coefficients using intuition and time-consuming iterations. The fuzzy-based method in [8] requires a trial-and-error procedure to make a rule table for implementation. As is widely known, this procedure requires a lot of time and expertise. When compared to existing strategies, the most prominent advantage of the proposed method is that it has only two design parameters and thus is very easy to tune.

Remark 2: A swing-up strategy which utilizes the

idea of letting the pendulum trajectory approach the orbit given by [4] was previously considered in [5]. The method in [5] is also based on a Lyapunov function, which includes the term \dot{x}^2 in addition to the term \dot{x}^2 . It is regarded that the paper intends to make $|x|$ converge to zero in addition to restricting it. However, the experimental results given in [5] show that x never converge to zero during the swing-up. Instead, x is biased to one side from the center. Furthermore, the swing-up time is very long. We don't need x to converge to zero for the swing-up. Instead, we want to restrict $|x|$. The cart's linear displacement $x(t)$ is given by $x(t) = \int_0^t \dot{x}(\tau) d\tau$ because the cart starts from the center of the rail. From this, we see that we can restrict $|x|$ by minimizing \dot{x}^2 . Therefore, we don't include the term x^2 in the Lyapunov function. Even though the Lyapunov function is similar to that in [5], the obtained control law is totally different from that of [5]. Furthermore, the proposed strategy has several features when compared to the method of [5]. First, the proposed control law is simple and has only two design parameters, while the control law in [5] requires four design parameters. This leads to easy tuning of design parameters as mentioned in Remark 1. Second, the stability procedure of the proposed method is much simpler. Third, the proposed method has a faster convergence rate. Finally, the proposed method shows good correspondence between simulation and experiment while the method in [5] does not. The last two features mentioned will be illustrated through simulations and experiments later in this paper.

Remark 3: Explicit representation of the relation between the parameter and the maximum value of x^2 is hardly available. Instead, we can say that increasing the parameter λ will reduce the value of \dot{x}^2 . This, in turn, will reduce $|x|$. This feature is well illustrated through the simulations and experiments of this paper.

4. STATE-DEPENDENT TRANSFORMATION FOR IMPLEMENTATION

The proposed swing-up strategy utilizes the acceleration of the cart, as given in (6), in order to swing a pendulum up. The inverted pendulum considered in this paper uses a DC motor as an actuator to move the cart. Therefore, the voltage input to a DC motor is a more appropriate control variable than the acceleration. We propose a state-dependent transformation in order to obtain a voltage input to a DC motor required to generate the acceleration given in (6). In order to derive the transformation, we first write the DC motor equation as follows:

$$I_m \ddot{\theta}_m + B_m \dot{\theta}_m = T_m - T, \quad (8)$$

where θ_m is the rotor angular displacement, I_m the rotor inertia, B_m a viscous-friction coefficient, T_m the

torque generated by a motor, and T the load torque that is used to move the cart through a timing pulley and a belt. The motor torque can be represented, as explained in [11], as

$$T_m = K_m i_a = K_m \left(-\frac{K_b}{R_m} \dot{\theta}_m + \frac{V_c}{R_m} \right), \quad (9)$$

where i_a is the winding current, K_m the torque constant, K_b the back-EMF constant, and V_c the voltage applied to a DC motor. The lab-built inverted pendulum system used in this paper utilizes a timing pulley and a belt in order to convert the rotational movement of a rotor to the translational movement. Let r be the radius of a timing pulley. Then x and θ_m are related as follows:

$$\dot{x} = r \dot{\theta}_m, \quad \ddot{x} = r \ddot{\theta}_m.$$

Utilizing the above relation, the motor torque given in (8) can be rewritten into

$$T_m = -\frac{K_m K_b}{R_m r} \dot{x} + \frac{K_m}{R_m} V_c. \quad (10)$$

From (8) and (10), we can represent the load torque as follows:

$$T = -\frac{I_m}{r} \ddot{x} - \left(\frac{B_m}{r} + \frac{K_m K_b}{R_m r} \right) \dot{x} + \frac{K_m}{R_m} V_c.$$

The force F exerted on the cart is given by

$$F = \frac{T}{r} = -\frac{I_m}{r^2} \ddot{x} - \left(\frac{B_m}{r^2} + \frac{K_m K_b}{R_m r^2} \right) \dot{x} + \frac{K_m}{R_m r} V_c. \quad (11)$$

Substituting F given in (11) into (2), we have the following dynamical equation:

$$\begin{aligned} \left(M + m + \frac{I_m}{r^2} \right) \ddot{x} - ml(\sin \theta) \dot{\theta}^2 + ml(\cos \theta) \ddot{\theta} \\ + \left(b + \frac{B_m}{r^2} + \frac{K_m K_b}{R_m r^2} \right) \dot{x} = \frac{K_m}{R_m r} V_c. \end{aligned} \quad (12)$$

From (1) and (12), we obtain

$$\ddot{x} = \frac{\Lambda_1 - \Lambda_2(\Lambda_3 + \Lambda_4 V_c)}{\Lambda_5}, \quad (13)$$

where

$$\begin{aligned} \Lambda_1 &= m^2 l^2 g \sin \theta \cos \theta, \\ \Lambda_2 &= \bar{I}_p, \\ \Lambda_3 &= -\left(b + \frac{B_m}{r^2} + \frac{K_m K_b}{R_m r^2} \right) \dot{x} + ml \sin \theta \dot{\theta}^2, \\ \Lambda_4 &= \frac{K_m}{R_m r}, \\ \Lambda_5 &= (ml \cos \theta)^2 - \bar{I}_p \left(M + m + \frac{I_m}{r^2} \right). \end{aligned}$$

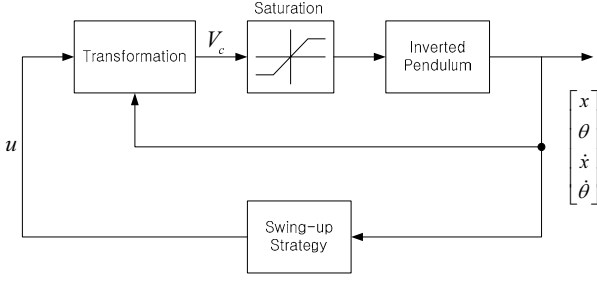


Fig. 3. Proposed control block diagram.

From (13), V_c and \ddot{x} are related as follows:

$$V_c = \frac{\Lambda_5 \ddot{x} - \Lambda_1 + \Lambda_2 \Lambda_3}{-\Lambda_2 \Lambda_4}. \quad (14)$$

Since $\ddot{x} = u$, the transformation is finally summarized into

$$V_c = \frac{\Lambda_5 u - \Lambda_1 + \Lambda_2 \Lambda_3}{-\Lambda_2 \Lambda_4}. \quad (15)$$

Fig. 3 depicts the proposed control method through a block diagram. Firstly, the cart's acceleration needed to swing up the pendulum is obtained from the proposed swing-up strategy and the obtained acceleration is fed to a state-dependent transformation in order to output the voltage value required to generate the required acceleration. Because the voltage to a DC motor is subject to saturation, i.e., $-V_{\max} \leq V_c \leq V_{\max}$, we need to decide design parameters u_a and λ such that the resulting V_c does not violate the voltage limit. Simulation study can be used for this purpose.

5. SIMULATION AND EXPERIMENT

In this section we provide simulation and experimental results in order to support the proposed swing-up strategy. Fig. 4 shows a lab-built cart pendulum system used in the experiment. The rail length is ± 0.45 m. The model parameters are given in Table 1. It is mentioned that some parameters that are not easy to obtain are assumed to have zero values. For example, see b , I_m , and B_m in Table 1. Even though we disregard those parameters, experimental results show that the proposed strategy still works well. Same parameter values were used in simulation study. Control strategy assumes that it switches from the nonlinear swing-up control law given

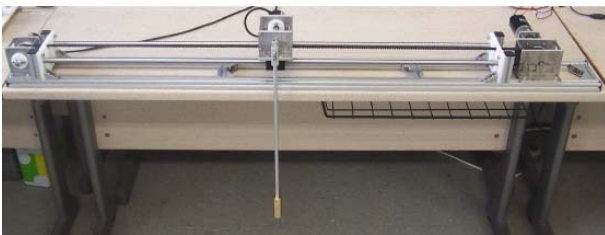


Fig. 4. Lab-built cart inverted pendulum.

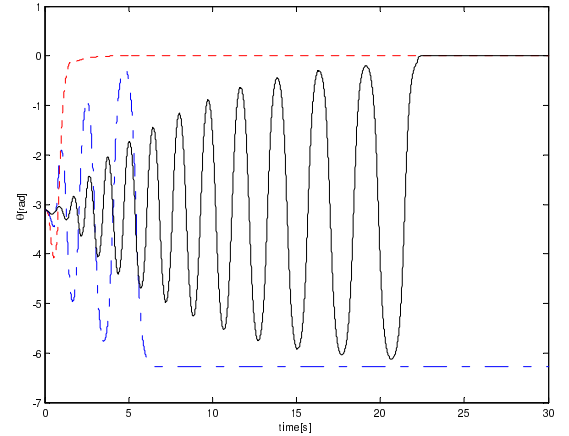
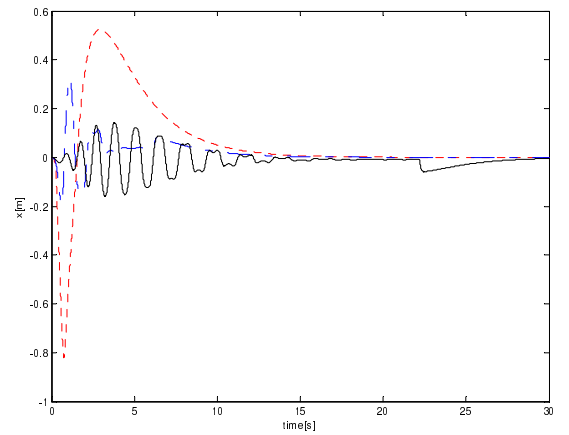
in (6) to a local linear controller if $|\theta| < 8^\circ$. We took $u_a = 5$ and performed simulation for three different values of λ . Figs. 5 and 6 compare the simulation results for the following initial condition:

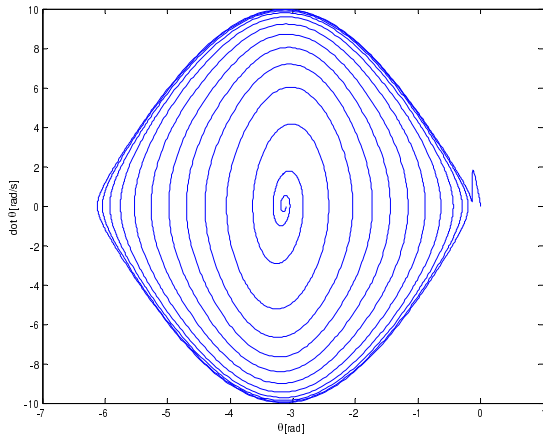
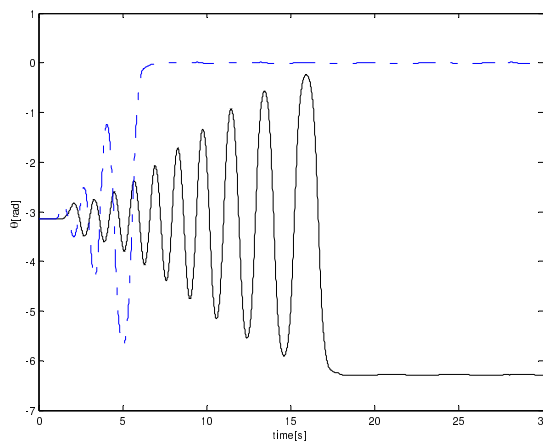
$$x = 0, \dot{x} = 0, \theta = -0.99\pi, \dot{\theta} = 0.$$

It is observed that the bigger the value of λ we use, the greater the number of swings needed to swing-up the pendulum to the upright position while the cart's

Table 1. Model parameters of the lab-built inverted pendulum.

Parameter	Value
\bar{I}_p	0.0267 kgm ²
M	0.711 kg
m	0.209 kg
l	0.326 m
B	0
I_m	0 kgm ²
B_m	0
r	0.0194 m
K_m	0.257 kgm ²
R_m	2.32 Ω

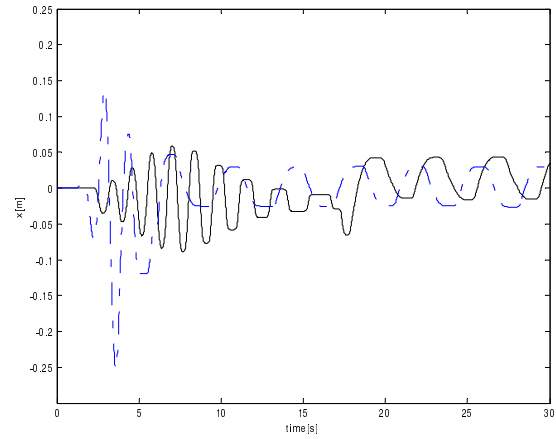
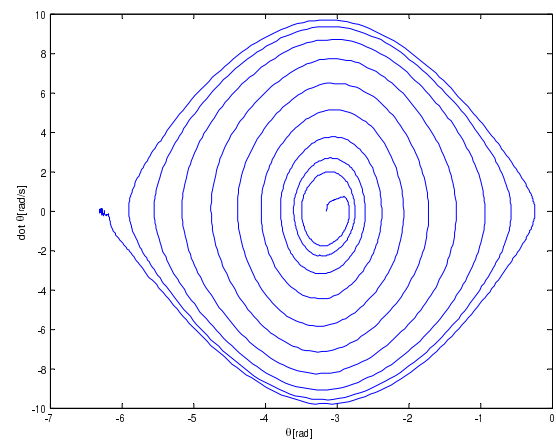
Fig. 5. Simulation result θ (dotted: $\lambda = 0.1$, dashdot: $\lambda = 2$, solid: $\lambda = 5$).Fig. 6. Simulation result x (dotted: $\lambda = 0.1$, dashdot: $\lambda = 2$, solid: $\lambda = 5$).

Fig. 7. Phase portrait for simulation: case of $\lambda = 5$.Fig. 8. Experiment result θ (dashdot: $\lambda = 2$, solid: $\lambda = 5$).

displacement remains in the smaller range. It is seen that the cart's displacement range for $\lambda = 0.1$ is beyond the rail limitation. This simulation example gives us a guide in deciding the design parameter λ . Fig. 7 shows the phase portrait drawn from the simulation result for the case of $\lambda = 5$. It is shown that the phase portrait approaches the orbit given by $E_p = 0$ as time goes.

As mentioned in Remark 2, Lozano's method [5] has a slow convergence rate. Simulation results given in [5] report that their strategy takes almost 120 seconds before switching to a linear controller. On the other hand, the proposed strategy takes less than 25 seconds for all three cases, which supports the notion that the proposed method has a faster convergence rate than the method shown in [5].

For comparison purposes, we performed experiments for two different values of λ . Unlike the simulation where the initial condition can be exactly specified, we hit the pendulum a little bit in the beginning to avoid the point $(\theta, \dot{\theta}) = (\pm\pi, 0)$. The experimental results given in Figs. 8 and 9 show the close resemblance with the simulation results, as mentioned in Remark 2. The oscillation of the cart's displacement after switching to a linear controller stems from the backlash of a gear used

Fig. 9. Experiment result x (dashdot: $\lambda = 2$, solid: $\lambda = 5$).Fig. 10. Phase portrait for experiment result: case of $\lambda = 5$.

in the DC motor. Note that, for $\lambda = 5$, the cart's displacement remains in the range ± 0.1 m during swing-up. Since the rail length is ± 0.45 m, the restriction on the rail length is well satisfied by the proposed swing-up strategy. Fig. 10 shows the phase portrait drawn from the experimental results for the case of $\lambda = 5$. From simulation and experiment, we see that we can satisfy the rail length limitation by adjusting a design parameter λ .

6. CONCLUSIONS

In this paper, we proposed a new swing-up strategy for inverted pendulums with restricted cart rail length. The proposed swing-up strategy is represented in a simpler form than existing swing-up strategies. The main advantage of the proposed method is that it has just two design parameters and thus is easy to tune. The cart's acceleration is considered as the control variable in the proposed method. However, the cart's acceleration cannot be directly manipulated. For implementation purposes, we provided a state-dependent transformation which yields voltage input to a DC motor required to generate the acceleration computed from the proposed swing-up strategy. The proposed swing-up strategy has been found to work well in simulation as well as

experimentally even though some model parameters are not carefully taken into account. We could affect the swing-up strategy by adjusting the design parameters such that the restriction on the rail length is satisfied.

REFERENCES

- [1] K. J. Astrom and K. Furuta, "Swinging up a pendulum by energy control," *IFAC 13th World Congress*, San Francisco, CA, 1996.
- [2] K. J. Astrom and K. Furuta, "Swinging up a pendulum by energy control," *Automatica*, vol. 36, no. 2, pp. 287-295, 2000.
- [3] Q. Wei, W. P. Dayawansa, and W. S. Levine, "Nonlinear controller for an inverted pendulum having restricted travel," *Automatica*, vol. 31, no. 6, pp. 841-850, 1995.
- [4] C. C. Chung and J. Houser, "Nonlinear control of a swinging pendulum," *Automatica*, vol. 31, no. 6, pp. 851-862, 1995.
- [5] R. Lozano, I. Fantoni, and D. J. Block, "Stabilization of the inverted pendulum around its homoclinic orbit," *System & Control Letters*, vol. 40, pp. 197-204, 2000.
- [6] J. Zhao and M. W. Spong, "Hybrid control for global stabilization of the cart-pendulum system," *Automatica*, vol. 37, no. 12, pp. 1941-1951, 2001.
- [7] D. Chatterjee, A. Patra, and H. K. Joglekar, "Swing-up and stabilization of a cart-pendulum system under restricted cart track length," *System & Control Letters*, vol. 47, pp. 355-364, 2002.
- [8] N. Muskinja and B. Tovornik, "Swinging up and stabilization of real inverted pendulum," *IEEE Trans. on Industrial Electronics*, vol. 53, no. 2, pp. 631-639, 2006.
- [9] F. Gordillo, J. A. Acosta, and J. Aracil, "A new swing-up law for the furuta pendulum," *International Journal of Control*, vol. 76, no. 8, pp. 836-844, 2003.
- [10] H. K. Khalil, *Nonlinear Systems*, 3rd edition, Prentice Hall, 2002.
- [11] B. C. Kuo and F. Golnaraghi, *Automatic Control Systems*, 8th edition, Wiley, 2003.



Ji-Hyuk Yang received the M.Sc. degree in Electrical Engineering from Inha University, Incheon, Korea, in 2008. He is currently pursuing a Ph.D. degree in Electrical Engineering at Inha University, Incheon, Korea. His primary research interest lies in the development of rapid control prototyping environment.



Su-Yong Shim received the B.Sc. degree in Electrical Engineering from Inha University, Incheon, Korea, in 2008. He is currently pursuing his M.Sc. degree in Electrical Engineering at Inha University, Incheon, Korea. His research interests are mechatronics and embedded systems.



Jung-Hun Seo received the B.Sc. degree in Electrical Engineering from Inha University, Incheon, Korea, in 2008. He is currently pursuing his M.Sc. degree in Electrical Engineering at Inha University, Incheon, Korea. His research interests are mechatronics, embedded systems, and control applications.



Young Sam Lee received the B.S. and M.S. degrees in Electrical Engineering from Inha University, Incheon, Korea in 1997 and 1999, respectively. He received the Ph.D. at the School of Electrical Engineering and Computer Science from Seoul National University, Seoul, Korea, in 2003. His research interests include time delay systems, receding horizon control, signal processing, and embedded systems. He is currently with the School of Electrical Engineering, Inha University, Incheon, Korea.